JOURNAL OF MATERIALS SCIENCE 17 (1982) 3140–3148

TEM observations of dislocation emission at crack tips in aluminium

J. A. HORTON, S. M. OHR
Solid State Division, Oak Ridge National Laboratory, Oak Ridge, Tennessee 37830, USA

Direct observations were made of the propagation of ductile cracks and associated dislocation behaviour at crack tips in aluminium during tensile deformation in an electron microscope. In the electropolished area, the cracks propagated as a Mode III shear-type by emitting screw dislocations on a plane coplanar to the crack plane. A zone free of dislocations was observed between the crack tip and the plastic zone. As the cracks propagated into thicker areas, the fracture mode changed from Mode III to predominantly Mode I. The crack top of the Mode I cracks was blunted by emitting edge dislocations on planes inclined to the crack plane. The blunted cracks did not propagate until the area ahead of the crack tip was sufficiently thinned by plastic deformation. The cracks then propagated abruptly, apparently without emitting dislocations. The stress intensity factor was measured from the crack tip geometry of Mode III cracks and it was found to be in good agreement with the critical value of the stress intensity factor required for dislocation generation.

1. Introduction

Direct observations by transmission electron microscopy have been made recently of the distribution of screw dislocations in the plastic zone of propagating cracks in various ductile and semibrittle metals and alloys [1–6]. It was found that screw dislocations were emitted from the crack tip on planes coplanar with the crack, and these dislocations were distributed in the plastic zone in the form of an inverse pile up. These represented the first direct observations of the distribution of dislocations in the plastic zone of shear cracks as predicted by Bilby *et al.* (BCS) [7]. More detailed examination revealed a dislocation-free zone (DFZ) between the crack tip and the inverse pile up. This situation has been analysed by Chang and Ohr [8, 9] who have shown that the length of the DFZ is directly related to the crack tip stress intensity factor K. Continued emission of dislocations and a correspondingly shorter DFZ will cause K to decrease to a point below the value K_g required for dislocation generation. Dislocation emission would then cease. These observations and the ensuing theoretical development have been concerned with shear cracks of either Mode II or Mode III type in which the crack tip remains sharp upon emitting dislocations.

The situation can be vastly different when the dislocations are emitted from Mode I cracks. Gilman [10] observed, by etch pit techniques, dislocation pile-ups on planes that are inclined to the crack plane. Cottrell [11] suggested that crack tip blunting could result from emission of edge dislocations on planes inclined at 45° to the crack. In the present work, direct observations have been made of the emission of such edge dislocations in aluminium during the propagation of Mode I cracks. The crack tip blunting processes are important since an increase in fracture toughness may result from the blunting.

The dislocation behaviour around the crack tip during crack blunting and crack propagation is affected by the presence of other dislocations such as those in cell walls formed during the early stages of plastic deformation. It has been reported previously that the cell walls can act as sources of dislocations in regions not associated with a crack and as sites for the nucleation of microcracks [12–14]. Detailed observations of these phenomena were made in aluminium during this investi-

0022–2461/82/113140–09$03.58/0

gation. It was found that the cell walls which crossed the plastic zone immediately in front of a crack tip dissolved by releasing all of their dislocations.

2. Experimental procedure

Tensile tests were performed in a Philips EM400T transmission electron microscope (TEM). Miniature tensile specimens (3 mm x 7 mm x 0.025 mm) were spark cut from 99.999% aluminium. Some of the specimens were prestrained 20% in order to develop a dislocation cell structure. These tensile specimens were electropolished until perforation in a 70% ethanol, 10% butyl cellusolve, 7.5% perchloric acid and 12.5% distilled water solution at 0° C. The region around the electropolishing hole was electron transparent while the edges of the specimens were of the original thickness.

The tensile stage for the TEM was hydraulically operated and had single-axis eucentric tilting. This pure tensile device was designed at ORNL [15]. Pressure in the hydraulic fluid was directly transferred into a pulling force on the specimen. This type of system could be operated as a constant load device. The tensile tests reported here were perfomed under constant load conditions. By using this method, an applied stress was still present after crack propagation or after plastic deformation had occurred and therefore the micrographs were made with the specimens under stress.

3. Results

During the TEM experiments, cracks originated at the edge of the electropolishing hole and propagated toward the thicker regions. In the thinnest areas next to the hole, the crack usually propagated along a straight path at 90° to the tensile axis with only a small amount of plastic deformation occurring. The character of the fracture process changed as the crack propagated into thicker regions. The cracks then followed a zigzag path averaging 90° to the tensile axis. The zigzag path was contained within a distinct plastic zone in front of the crack which had undergone significant thinning due to plastic deformation processes. The region in front of the crack tip always thinned sufficiently for observations with 100 keV electrons.

In order to determine the operative bulk fracture mode, scanning electron microscopy (SEM) was performed on the fracture surface of a specimen previously deformed until it had fractured completely in the TEM. The thick, originally not electropolished, shoulder region was examined. The specimens failed by a ductile chisel-edge fracture mode. Plastic deformation processes continued until a sharp chisel edge was produced. Thin ligaments were observed protruding along this edge. The actual fracture occurred as a crack propagated in a zigzag fashion through these ligaments.

It is this fracture process which was observed when performing a tensile experiment inside a TEM. Fig. 1 shows a scanning electron micrograph and a TEM micrograph at the same magnification of the ligaments produced during deformation of a 0.25 mm thick aluminium specimen. The SEM micrograph is nearly an edge-on view; it shows that the specimen had undergone substantial necking before fracture and shows the ligaments which were produced along the fracture edge. The TEM micrograph is a top view of a similar region of the same specimen and shows that the ligaments were electron transparent. At the base of the ligament indicated by the arrow in the TEM micrograph in Fig. 1, the thickness was determined to be 390 nm. This was determined by the number of fringes present and confirmed by convergent-beam electron diffraction.

As previously mentioned, the cracks propagated

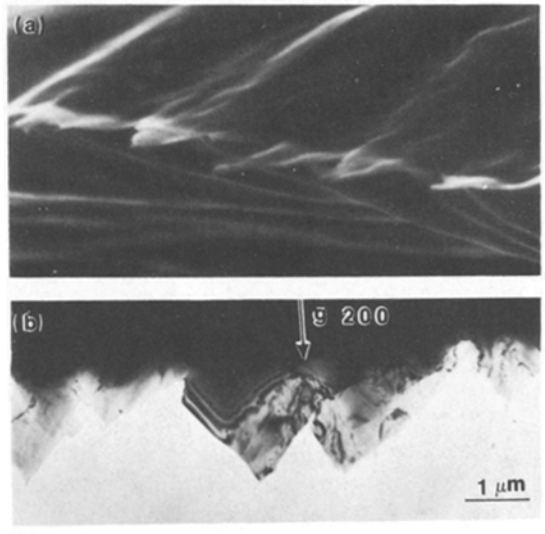

Figure 1 (a) SEM and (b) TEM micrographs of an aluminium specimen tensile tested inside the TEM. (a) is an end-on view showing ligaments which were formed during the final stage of fracture and (b) is a top view. In (b) the electron beam direction, B, was near [013].

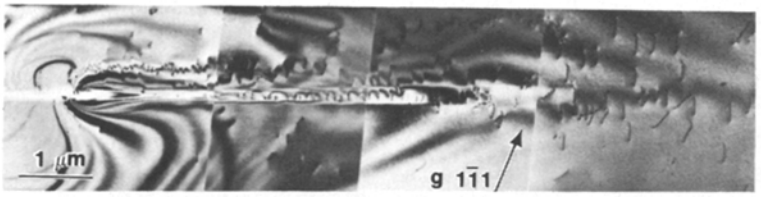

Figure 2 TEM micrograph of a pile-up of screw dislocations ahead of a Mode III crack propagation during *in situ* tensile deformation in aluminium. B near [011], the foil normal (FN) is near [125], and the slip system is $a/2[101]$ $(\bar{1}11)$.

in a straight path in the regions which were orignally electron transparent. This is shown in Fig. 2. The crack emitted screw dislocations on a plane coplanar with the crack. The generalized plastic deformation which normally led to thinning in front of the crack was absent in this already thin region. Since the crack flanks were displaced nearly perpendicular to the plane of the specimen, as measured by stereoscopic observation, it was determined that the crack propagated as a Mode III shear crack in this region. The dislocation distribution shown in Fig. 2 appeared similar to previous observations for other materials [5]. Past observations in fcc metals have shown a distinct DFZ and an inverse pile up of dislocations. As shown in Fig. 2, a DFZ was present in front of the crack tip. The dislocations did not form an inverse pile up as distinctly as was observed in the other fcc materials. This may be due to the fact that aluminium is a metal of high stacking fault energy and hence the dislocations are not split into partials. The dislocations cross-slipped out of the slip plane after they were generated from the crack tip, forming a plastic zone which was broader than those found in metals of low stacking fault energy. The distribution of dislocations in aluminium is similar to that found in the plastic zone of bcc metals [4].

Upon further deformation the crack propagated into the thicker regions which initially were not electron transparent. The basic fracture mode, as determined by the separation of the crack flanks, changed from Mode III to predominantly Mode I in the thicker regions. The crack propagated in a zigzag fashion within the plastic zone producing the ligaments shown in Fig. 1. During this crack propagation the dislocations emitted by the crack tips were generally not on planes coplanar with the cracks and were usually emitted on slip planes which ranged 45° to 90° to the crack propagation direction. This process was repeatedly observed as the crack propagated into the specimen. Fig. 3

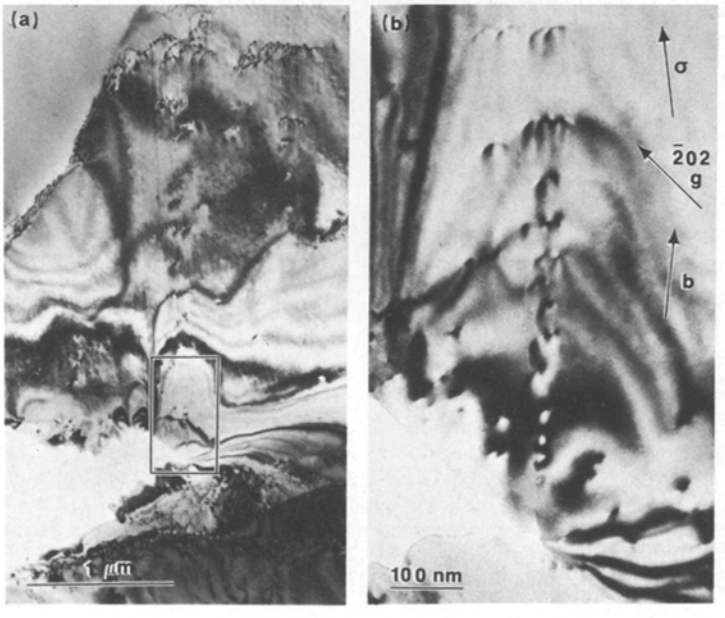

Figure 3 TEM micrographs of edge dislocations emitted from a crack tip during Mode I crack propagation. (b) is at a higher magnification than (a) and is at a slightly different tilt so that the same g was the operating reflection. Note the tensile axis and projected Burgers vector direction are perpendicular to the crack propagation direction. The operative slip system was $a/2[0\bar{1}1]$ (111), B near [101], FN near [233].

shows an area in which the dislocations were emitted perpendicular to the crack propagation direction. A cell wall in the upper part of the low-magnification micrograph (Fig. 3a) impeded the motion of the dislocations. For Fig. 3b, the foil was tilted slightly (as compared to the orientation used for Fig. 3a) in order to bring the dislocations nearer the crack tip into contrast. The dislocations had $a/2[0\bar{1}1]$ Burgers vectors, resided on (1 1 1) slip planes, and were primarily edge in character. The tensile axis, Burgers vector and direction of dislocation motion were all nearly 90° to the crack, which is consistent with Mode I crack geometry.

As was mentioned earlier, the Mode I crack always propagated within the plastic zone which was thinned appreciably by plastic deformation and was usually at 90° to the tensile axis. The crack generally propagated abruptly with no apparent dislocation emission. This forward propagation followed a zigzag path through the plastic zone. For a short interval, the crack propagated at about 45° to the tensile axis toward the side of the plastic zone. As the crack propagated into this thicker region, the crack either changed direction back toward the centre of the plastic zone, where it was thinnest, or stopped propagating. The crack propagated much faster than the rate at which the area ahead of the crack tip was thinned by plastic deformation so that the crack eventually came to a stop.

During the propagation, the crack tip was always sharp. However, as the crack was arrested the crack tip blunted immediately by emitting dislocations. This can be seen in Fig. 3. As shown in Fig. 4, the crack tip sometimes blunted only slightly, then propagated forward a short distance and blunted again by emitting edge dislocations

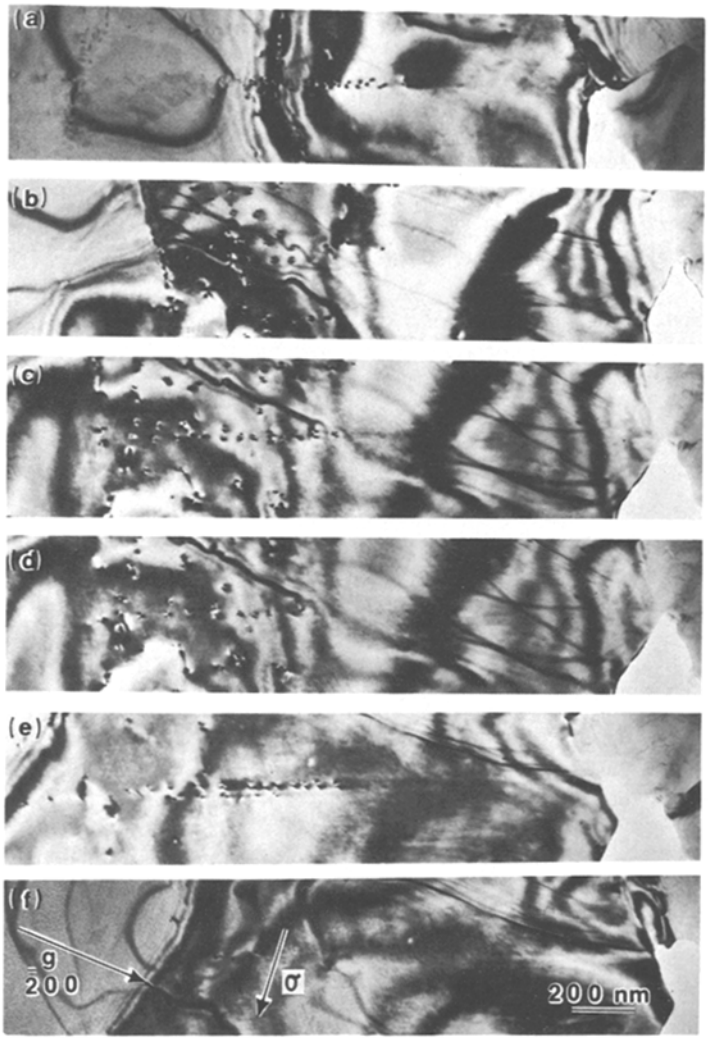

Figure 4 Sequential TEM micrographs showing dislocation emission during the crack-tip blunting process. Between (b) and (d) the crack has blunted by emitting edge dislocations while not propagating forward. B near [011], FN near [345].

on a parallel plane. Usually, the blunting continued until the crack tip reached a width of the order of one micrometre. This may be described as a "sliding off" process. As shown in Fig. 3, the dislocations were emitted along one side of the crack and hence the crack tip maintained a sharp corner at the site of dislocation emission. Eventually, the crack tip formed a nearly square front and the dislocation activity ceased. When the material in front of the crack thinned sufficiently with additional deformation, a new sharp crack was initiated at some point along the blunted crack front and abruptly propagated forward.

The process of crack blunting by dislocation emission on parallel slip planes is shown in a sequence of six micrographs in Fig. 4. The specimen was under constant load during this sequence of micrographs. It can be seen that the crack propagated slightly between Micrographs a and b, d and e, and e and f. The sequence in Fig. 4b, c, and d shows the crack blunting process in which edge dislocations were emitted on slip planes at an angle of about 90° to the crack. The crack did not propagate forward but only blunted and all the dislocations were emitted within a narrow layer of slip planes. These slip planes intersected the exact crack tip as determined by extending a line intersecting the dislocations in the pile up toward the crack. Between Micrographs b and d, the crack tip increased in width by about 25 nm. Micrograph e shows that the crack tip dislocations were emitted on a new set of slip planes as the crack propagated forward. The remnants of the last pile up are still evident in this micrograph which shows that they resided adjacent and parallel to the new set. The diffraction contour between the crack tip and the first dislocation was the same [200] contour that was present in the region of the dislocation pile up. During deformation the dislocations suddenly appeared in the centre area of the micrographs and then moved at an observable rate away from the crack tip. Since the entire area had the same contour in contrast, if a dislocation of the same Burgers vector was in the region between the crack tip and the first dislocation, it should have been in contrast. The dislocations apparently travelled through the dislocation-free zone (DFZ) at a rate too rapid to be observed. The appearance of the DFZ and the pile up of these dislocations was similar to that shown in Fig. 2 of screw dislocations generated by a Mode III crack, although the pile up in Fig. 4 was on a much smaller scale. As can be seen in Fig. 4f, many of the edge dislocations generated at the crack tip of Mode I cracks moved out of the crack tip area, leaving behind only a small number of dislocations compared to Mode III cracks. At this point a new crack initiated along the side of the ligament and abruptly propagated in a zigzag fashion through the region shown in Fig. 4.

Throughout the experiments, the dislocations were observed to originate from the crack tip, from cell walls which crossed the plastic zone and from the thick regions of the crack flank. An example of the dissolution of cell walls ahead of a Mode III crack is shown in a sequence of four micrographs in Fig. 5. Two cell walls crossed the plastic zone near the left of Fig. 5a. The crack tip is located to the right of the micrograph and the plastic zone extends straight into the specimen area shown. The plastic zone is outlined by the lines on the micrograph which delineate the intersections of the active slip plane and the surface. As the specimen was deformed (Fig. 5b), dislocations which originated at the crack tip travelled through this plastic zone. The dislocations were bowed away from the crack tip due to the applied stress. The cell walls have partially dissolved in Fig. 5b and the dislocations were able to travel through the cell walls. The Burgers vector was determined to be $a/2[10\bar{1}]$ by performing a contrast analysis as shown in Fig. 5c, where the bowed dislocations are out of contrast for a diffraction vector, g, equal to $[\bar{1}1\bar{1}]$. The dislocations were found to be primarily of screw character and hence the crack was a shear crack of Mode III type. The projection of the Burgers vector on to the specimen plane and the tensile axis are indicated on Fig. 5d. In Fig. 5d the cell walls have further dissolved as more dislocations have traversed the region

Cell walls were also observed to dissolve in front of a crack tip during edge dislocation emission on planes inclined to the crack plane. In this case, the thinning process in front of the crack tip resulted from a more generalized deformation than that shown in Fig. 5. After the cell wall completely disappeared and the resulting dislocation density in the ligament became relatively low, the crack propagated through the ligament. The plastic zone more than doubled in width, which corresponded to a local strain of at least 100%. The cell walls also provided sites for microcrack

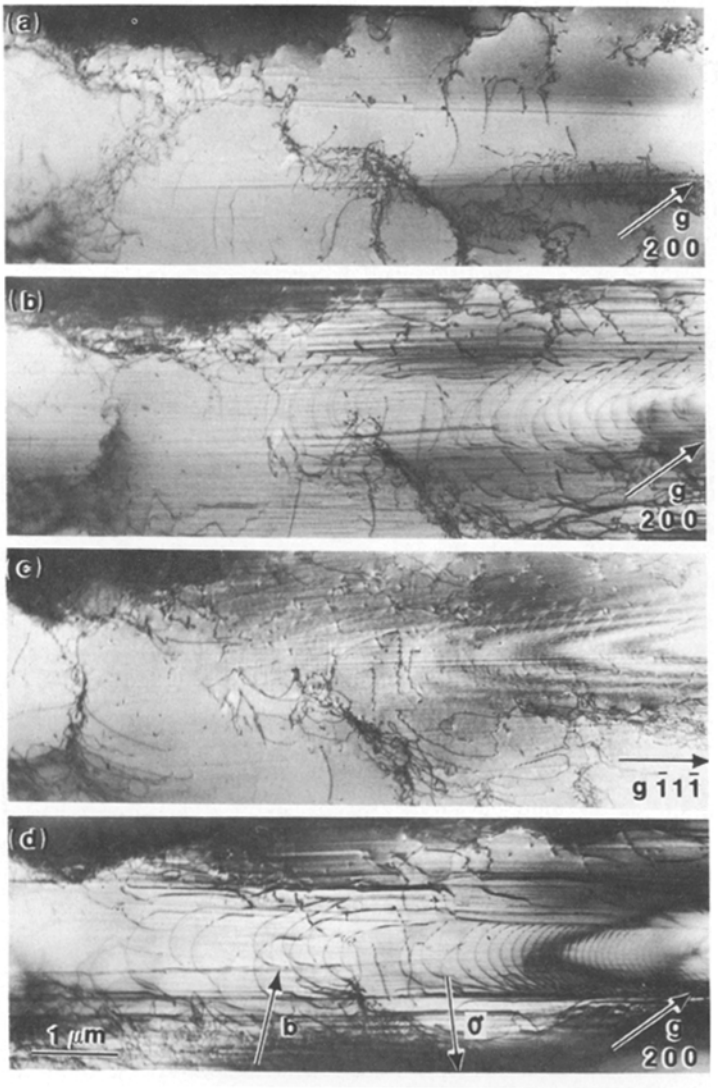

Figure 5 Sequential TEM micrographs of cell wall dissolution during the passage of crack tip generated screw dislocations. The slip system was $a/2[10\bar{1}]$ $(1\bar{1}1)$, B near [012] (except for (c)), FN near [125].

nucleation ahead of the main crack. This observation has been reported before, based on tensile experiments in beryllium, by Gardner *et al.* [12].

4. Discussion

The TEM observations of crack tip phenomena in aluminium reported here showed two distinct modes of crack propagation, namely Modes I and III, with corresponding dislocation behaviour at the crack tip. In the electropolished thin areas next to the hole, shear cracks of Mode III type propagated by emitting screw dislocations on planes coplanar with the cracks. The crack tip displacement had a large component in the direction perpendicular to the plane of the specimen, which is consistent with a Mode III crack tip geometry. The crack tip remained sharp during this mode of propagation. As the cracks moved into the thicker part of the specimen, the crack tip area became electron transparent due to plastic deformation. In this region, the cracks propagated predominantly by Mode I with the crack tip displacement nearly perpendicular to the plane of the crack. The Mode I cracks were often blunted by emitting edge dislocations on inclined planes. These observations are in general agreement with the dislocation model of Mode I cracks, originally proposed by Bilby and Swinden [16] and subsequently refined by Vitek [17] and Reidel [18]. In these models, the plastic zone consists of edge dislocation pile ups on inclined

planes and the crack is blunted by emitting dislocations.

The observed change in the fracture mode from Mode III to Mode I between the thin electropolished area and the originally thicker area may be attributed to the loading geometry. In the electropolished area, the thickness of the specimen was thin both in the vicinity of the crack tip and in the neighbouring areas, so that a plane stress condition was established. This state of stress led to shear crack propagation by a Mode III mechanism. As the crack moved into the thicker area, the state of stress approached plane strain conditions in the general area surrounding the crack, which constrained the specimens from being displaced in the direction perpendicular to the direction of crack propagation. This situation then favoured crack propagation in Mode I.

During Mode I crack propagation, in the originally thicker regions of the specimen, the cracks either blunted by emitting edge dislocations or the cracks propagated abruptly forward. During the blunting phase, the cracks on both a microscopic scale met the generally defined geometric criteria associated with Mode I fracture. If only one set of edge dislocations is emitted on an inclined plane and if that angle is near 90° to the crack then the crack does not actually propagate forward but only blunts. This was the situation observed repeatedly. A sharp corner was maintained from which the edge dislocations were emitted. As was pointed out by Cottrell [11], a characteristic of Mode I cracks is that fresh dislocations must be generated at the crack tip in order to provide the crack-opening displacement if a crack is to propagate by plastic deformation. This process is termed noncumulative, in contrast to the situation predicted for shear fracture of Modes II and III where the dislocations moving in front of the crack contribute continuously to the crack-opening displacement. Since a shear fracture is usually expected for ductile failure, our observation is somewhat surprising that Mode I dominates over Mode III during fracture of aluminium.

The condition for the generation of dislocations from a Mode I crack was discussed by Rice and Thomson [19]. By balancing the crack-tip stress field due to the applied stress, the image stress and the ledge stress, they derived the critical distance at which the stress on a dislocation vanished. It was proposed that, if this critical distance is less than the core radius of the dislocation, the crack will be blunted by generating dislocations. Using this criterion, most fcc metals including aluminium are expected to generate dislocations spontaneously from the crack tip. Their prediction is therefore in agreement with our observation in aluminium that arrested Mode I cracks always blunted by emitting edge dislocations on inclined planes.

The emission of edge dislocations and subsequent blunting of a crack tip are influenced by the local shear stress and the available slip systems. The shear stress, $\sigma_{r\theta}$, near the crack tip of a Mode I crack on an inclined slip plane is given by

$$\sigma_{r\theta} = \frac{K_I}{(2\pi r)^{1/2}} \sin\left(\frac{\theta}{2}\right) \cos^2\left(\frac{\theta}{2}\right) \quad (1)$$

where K_I is the Mode I stress-intensity factor, r is the distance from the crack tip and θ is the angle between the slip plane and the crack plane. The shear stress has a broad maximum between $\theta = 40$ to 90° with an actual maximum occurring at $\theta = 70.5°$. The present observation that the edge dislocations are emitted on planes between 45° and 90° from the crack plane is, therefore, in agreement with the angular dependence of the shear stress near the crack tip. The angle of inclination for a given crack will depend on the crystallographic orientation of the crack and hence on the Schmid factor of available slip systems.

The crack blunting usually continued until the crack front became nearly square. The amount of plastic deformation contributed by the blunting dislocations, however, was very small compared to the overall plastic deformation which occurred throughout the specimen. The blunted crack did not propagate until the material ahead of the crack tip was thinned by plastic deformation. When the ligament in front of the crack was sufficiently thin, the crack propagated by nucleating a sharp crack without any apparent dislocation emission. This final step must be considered as an elastic fracture rather than plastic fracture. Thus the process of crack propagation apparently depends on a critical thickness being reached during the thinning of the ligament. It was sometimes found that a microcrack was nucleated in front of an existing crack so that a ligament was formed between the crack and the microcrack and the crack propagated by breaking the ligament and coalescing with the microcrack.

The present TEM observations of dislocation motion near crack tips were made during ligament failure along the chisel edge pronounced by plastic deformation. Ligament failure is part of the microvoid coalescence or dimple rupture mode of fracture which occurs by a process of void nucleation, void growth, and final fracture through the walls or ligaments between the cavities. Actual crack propagation occurs in these ligaments. It is this final stage in the process which can be directly observed in the TEM during *in situ* deformation. The cavity–crack tip interactions have been studied by this TEM technique by Horton *et al.* [20] in which it was shown that screw dislocations generated by the crack tip cut, sheared and elongated voids without casuing a void volume enlargement.

The theory of Bilby *et al.* [7] has been recently extended to treat a linear distribution of dislocations with a DFZ at the crack tip of Mode III shear cracks [8, 9]. One of the results of this analysis is an expression relating the stress intensity factor K at the crack tip to the crack tip geometry:

$$\frac{K}{\sigma_f\sqrt{c}} = \frac{2(e^2 - c^2)}{e} F(\pi/2, k^2) \qquad (2)$$

where σ_f is the friction stress, c is the crack length, e is the crack plus DFZ length, F is the elliptic integral of the first kind where the modulus k^2 is given by

$$k^2 = \frac{(a^2 - e^2)c^2}{(a^2 - c^2)e^2}$$

and a is equal to e plus the plastic zone length. It was shown that K is proporational to the size of the DFZ. As the size of the DFZ vanishes ($e \to c$), the crack approaches the BCS crack for which the stress intensity factor K is zero. It was shown that the presence of a DFZ is associated with the difficulty in generating dislocations at the crack tip. More specifically, a DFZ is expected if there is a critical stress intensity factor K_g required for dislocation generation at a crack tip. Based on the dislocation generation model of Rice and Thomson [19] the expression for K_g was obtained as

$$K_g^2 = \frac{\pi A^2}{2r_c} \qquad (3)$$

where $A = \mu b/2\pi$ for a screw dislocation pile up. μ is the shear modulus, b is the Burgers vector and r_c is the dislocation core radius.

We have analysed the geometry of the DFZ and the plastic zone of the Mode III crack shown in Fig. 2 based on the DFZ theory of fracture. Experimentally we have $c = 19.1\,\mu m$, $e = 21.2\,\mu m$, $a = 26.7\,\mu m$. Following the suggestion of Bilby *et al.* [7] and the more recent finding of Prinz *et al.* [21], we have used for the friction stress the yield stress (20.0 MPa) as determined from bulk tensile tests for this material. From Equation 2, the stress intensity factor K is then found to be $K = 0.85 \times 10^5\ N m^{-3/2}$. This experimental value of K may be compared with the value of $k_g = 0.6 \times 10^5\ N m^{-3/2}$ for dislocation generation calculated using Equation 3 and with $K_{IIIc} = (4\mu\gamma)^{1/2} = 2.9 \times 10^5\ N m^{-3/2}$ for brittle fracture, where γ is the surface energy and was assumed to have a value of $0.84\ J m^{-2}$ for aluminium. It can be seen that the experimental value of K is in good agreement with the value of K_g. It suggests very strongly that the stress intensity factor at the tip of a Mode III crack is determined by the critical value of K required for dislocation generation. As the stress is applied externally, the magnitude of K at the crack tip increases. In ductile materials such as aluminium, K_g is less than K_c so that K reaches K_g first and the dislocations are generated at the crack tip. Since the plastic deformation relaxes the stress field at the crack tip, K cannot increase any further even if the applied stress is increased. Thus, it is expected that K at the crack tip remains at K_g and the number of dislocations in the plastic zone increases with increasing applied stress. This will lead to material failure in a ductile manner involving void growth and necking. The criterion of ductile versus brittle fracture based on the relative magmitude of K_g versus K_c presented here was originally proposed by Rice and was reported by Mason [22]. The analysis of the crack tip geometry of Mode I cracks was not carried out in the present work because the DFZ theory available at present is only applicable to shear cracks of Modes II and III.

5. Summary

(a) Thin sheets of pure aluminium (up to 0.25 mm thick) failed by a ductile chisel-edge fracture mode, and along the fracture edge very thin ligaments were produced which were transparent to 100 kV electrons. The actual crack followed a zigzag path through these ligaments.

(b) In thin areas, cracks emitted screw dislocations on planes coplanar with the crack (Mode

III). These dislocations formed an inverse pile up and exhibited a zone free of dislocations at the crack tip. This observation extends previous observations in fcc metals to a metal with a higher stacking fault energy.

(c) In thicker areas, dislocations of primarily edge character were emitted from crack tips on planes inclined to the crack plane (Mode I). This dislocation emission led to blunting of the crack tip and also resulted in a dislocation-free zone next to the crack tip.

(d) The Mode I crack which is blunted by emitting dislocations does not advance until the area ahead of the crack tip is sufficiently thinned by plastic deformation. The crack then propagated without emitting dislocations.

(e) Dislocation cell walls which crossed the plastic zone provided dislocations to assist the thinning process. These cell walls usually totally disintegrated resulting in a relatively dislocation-free ligament. Sometimes these cell walls acted as sites for microcrack initiation ahead of the main crack.

(f) The stress intensity factor K was measured from the observed lengths of the crack, the dislocation-free zone and the plastic zone of Mode III cracks. The value of K was in good agreement with the critical value of K required for dislocation generation.

Acknowledgements

The authors wish to thank F. W. Young, Jr, for his continuing interest and for reviewing this manuscript. The authors also wish to acknowledge the helpful discussions with S.-J. Chang and the technical assistance of T. C. Estes and C. W. Boggs. The research was sponsored by the Division of Materials Sciences, US Department of Energy, under Contract W-7405-eng-26 with Union Carbide Corporation. This article is published by kind permission of the US Government ©.

References

1. J. NARAYAN and S. M. OHR, Proceedings 9th International Congress on Electron Microscopy, Vol. 1, Edited by J. M. Sturgess (1978) p. 580.
2. S. KOBAYASHI and S. M. OHR, Proceedings 37th Annual Meeting of EMSA, Edited by G. W. Bailey (1979) p. 424.
3. S. M. OHR and J. NARAYAN, *Phil. Mag.* **A41** (1980) 81.
4. S. KOBAYASHI and S. M. OHR, *ibid.* **A42** (1980) 763.
5. S. M. OHR and S. KOYAYASHI, *J. Metals* **32** (1980) 35.
6. S. KOBAYASHI and S. M. OHR, *Scripta Met.* **15** (1981) 343.
7. B. A. BILBY, A. H. COTTRELL and K. H. SWINDEN, *Proc. R. Soc.* **A272** (1963) 304.
8. S.-J. CHANG and S. M. OHR, in "Dislocation Modelling of Physical Systems", Edited by M. F. Ashby, R. Bullough, C. S. Hartley and J. P. Hirth (Pergamon Press, New York, 1981) p. 23.
9. S.-J. CHANG and S. M. OHR, *J. Appl. Phys.* **52** (1981) 7174.
10. J. J. GILMAN, *J. Met.* **9** (1957) 449.
11. A. H. COTTRELL, *Proc. R. Soc.* **A285** (1965) 10.
12. R. N. GARDNER, T. C. POLLOCK and H. G. F. WILSDORF, *Mater. Sci. Eng.* **29** (1977) 169.
13. T. IMURA, Proceedings of the US–Japan Seminar on New Applications and Extensions of the Unique Advantages of HVEM for Physical and Materials Research, University of Hawaii, Honolulu (1976).
14. H. G. F. WILSDORF and D. KUHLMANN-WILSDORF, *Norelco Reporter* **5** (1958) 9.
15. J. A. HORTON, Proceedings of the 40th Annual Meeting of EMSA, edited by G. W. Bailey (1982) in press.
16. B. A. BILBY and K. H. SWINDEN, *Proc. R. Soc.* **A285** (1965) 22.
17. V. VITEK, *J. Mech. Phys. Solids* **24** (1976) 263.
18. H. REIDEL, *ibid* **24** (1976) 277.
19. J. R. RICE and R. THOMSON, *Phil. Mag.* **29** (1974) 73.
20. J. A. HORTON, S. M. OHR and W. A. JESSER, *J. Nucl. Mater.* in press.
21. F. PRINZ, H. P. KARNTHALER and H. O. K. KIRCHNER, *Acta Met.* **29** (1981) 1029.
22. D. D. MASON, *Phil. Mag.* **A39** (1979) 455.

Received 17 February
and accepted 16 March 1982